Structural Characterization of Complexes between Iminodiacetate Blocked on Styrene−Divinylbenzene Matrix (Chelex 100 Resin) and Fe(III), Cr(III), and Zn(II) in Solid Phase by Energy-Dispersive X-ray Diffraction

D. Atzei,[†] T. Ferri,[‡] C. Sadun,[§] P. Sangiorgio,[‡] and R. Caminiti*[,§]

Contribution from the Dipartimento di Chimica, INFM Istituto Nazionale di Fisica della Materia, Università degli Studi di Roma "La Sapienza", Ple A. Moro 5, 00185 Roma, Italy, Dipartimento di Chimica, Università degli Studi di Roma "La Sapienza", Ple A. Moro 5, 00185 Roma, Italy, Dipartimento di Chimica Inorganica e Analitica, Università di Cagliari, Complesso Universitario di Monserrato, SS 554 Bivio per Sestu, 09042 Monserrato (CA), Italy

Received February 1, 2000. Revised Manuscript Received July 25, 2000

Abstract: Local structure of Fe(III), Cr(III), and Zn(II) cations has been determined on the amorphous sample by means of the *difference method* used for liquid systems. We recorded energy-dispersive X-ray diffraction spectra of a chelating resin (Chelex 100), containing paired iminodiacetate ions coupled to a styrene-divinylbenzene support, in several ionic forms. Coordination geometry of Fe(III), Cr(III), and Zn(II) metal cations with Chelex 100 resin ligand sites, and conformation of the ligand groups have been determined.

Introduction

A knowledge of the all of the constituents of a sample does not suffice to assess its environmental hazard because the metals can be present in a variety of forms. Trace metals analysis is gaining increasing attention now that it is widely acknowledged that trace elements play a fundamental role in the metabolism of living organisms. It is essential to know both content and chemical form of each species present in the matrix (speciation), because bioavailability and toxicity depend strongly thereon.

Analytical techniques are becoming increasingly reliable and sensitive, though the presence of interfering species may create problems in metal determination. Thus, a preliminary separation step (clean-up) is required, or the metal must be isolated from the matrix.

Chelating ion-exchange resins is one of the most powerful and widely used systems for achieving this separation/preconcentration step. Chelating polymers differ from ion-exchangers in their high selectivity, bond strength, and kinetics. For this reason, chelating resins can be advantageously used to study trace metals and their speciation,[1−4] thus allowing the determination of low metal concentrations not otherwise detectable by direct measurements. This kind of resin is widely employed also for separating small molecules as organic acid, nucleic acid, and carbohydrates.

Chelex chelating resin is classed among the weak acid cation-exchange resins by virtue of its carboxylic acid groups, but it differs from ordinary exchangers in its high selectivity for metal ions and its much greater bond strength.

Chelex chelating resin operates in basic, neutral, and weakly acidic solutions at pH 4 or higher. At very low pH, the resin acts as an anion exchanger. Its structure changes with increasing pH. At pH ranging from 2.21 to 3.99 the cationic form is the dominant form, the iminodiacetate (IDA) group is in NH^+-form, and the ligand can be expressed as ($-LH_3^+$). At pH between 3.99 and 7.41, the zwitterionic form is dominant, with the IDA group in the NH^+COO^- form ($-LH_2$). At pH over 7.41 and up to 12.30, the monovalent anionic form prevails ($-LH^-$), and only over pH 12.30 is the stable form the divalent anionic form[5] ($-L^{2-}$).

Another feature of the Chelex 100 resin is that its volume changes when its ionic form is altered. The water uptake, or swelling, is especially pronounced because of its low cross-linking. In water, the volume of hydrogen form and multivalent ionic forms do not differ substantially as one passes to a monovalent salt form.[5]

Because of their importance in analytical techniques, IDA chelating resins have been widely studied. Absorption kinetics, pH absorption, and selectivity order toward metal ions have been defined.[5−8] Actual selectivity values for any particular system depend on pH, ionic strength, and the presence of other complex-forming species. The selectivity factor is a quantitative measure of the affinity that the Chelex resin displays for a particular cation as compared to its affinity for a reference cation. The selectivity of Chelex resin toward metal cations does not compare to that of IDA ligands in solution. This feature has been qualitatively ascribed to the polymer effect[7] or ion

* To whom correspondence should be addressed. E-mail: r.caminiti@caspur.it.
[†] Università di Cagliari.
[‡] Università degli Studi di Roma "La Sapienza".
[§] INFM Istituto Nazionale di Fisica della Materia.

(1) Florence, T. M.; Batley, G. E. *CRC Crit. Rev. Anal. Chem.* **1980**, *9*, 219.
(2) Ferri, T.; Sangiorgio, P. *Anal. Chim. Acta* **1996**, *321*, 185.
(3) Ferri, T.; Minelli, L.; Rossi, S.; Sangiorgio, P. *Ann. Chim. (Rome)* **1996**, *86*, 1996.
(4) Hill, S. J. *Chem. Soc. Rev.* **1997**, *26*, 291−298.
(5) Schmuckler, G. *Talanta* **1965**, *12*, 281−290.
(6) Schmuckler, G. *Talanta* **1963**, *10*, 745−751.
(7) Kantipuly, C.; Katragadda, S.; Chow, A.; Gesser, H. D. *Talanta* **1990**, *37* (5), 491−517.
(8) Yuchi, T.; Sato, Y.; Morimoto, H.; Mzuno, H.; Wade, H. *Anal.Chem.* **1997**, *69*, 2941−2944.

10.1021/ja0003728 CCC: $20.00
Published on Web 02/22/2001

exchange effect, as well as complexation reactions.[9] Several studies of coordination of the IDA ligand in solution and in the crystal state have been carried out recently, but no structural information is available for an IDA group included in a polymeric matrix (chelating resins). Several IDA group coordination modes could be hypothesised. IDA could use all three of its donor atoms, as free ligands do, or it could use only one or two atoms. It may be assumed that different species, namely the 1−1, 1−2, 1−3 complexes, can be obtained.

Structural information, as in many other areas of materials science, is essential to gain an understanding of the samples' physical behavior. The major difficulties in determining the coordination structure of a metal ion with a chelating resin lie in its highly complex amorphous structure. In this case, wide-angle X-ray diffraction (WAXS) is particularly well-suited for providing insight into the way cations interact with their surroundings.

The coordination geometry of several metal ions in the amorphous state has been studied using this technique.[10−12] Here we used the difference method[13,14], successfully applied to liquid systems, for treating experimental WAXS data, and we assumed that resin structure is not altered by metal ions absorption. The cations maintain the electroneutrality of the polyion matrix by confining their distribution to the volume of the beads. In this way, the radial distribution function of Chelex 100, in hydrogen form such that H^+ maintains electroneutrality, can be subtracted from the radial distribution function of the loaded resin. By so doing, the contributions of metal-ion−resin and metal-ion−metal-ion interactions remain.

The difference method of neutron diffraction and isotopic substitution (NDIS) has been applied by R. H. Tromp and G. W. Neilson[15] to aqueous (D_2O) poly(styrene-sulfonate) ion-exchange resins with Ni(II) and Li(I).

Experimental Section

Equipment. The X-ray diffraction experiments were carried out using a noncommercial X-ray energy scanning diffractometer.[16,17] The diffractometer consisted of (1) a Seifert X-ray generator, (2) a water-cooled tungsten X-ray source with 3.0 kW maximum power (the bremsstrahlung component of the X-ray source was used), (3) a germanium solid-state detector (SSD) connected to a multichannel analyzer by an electronic chain for diffraction spectra collection, (4) a collimator system which focuses the X-ray beam in front of and behind the sample, (5) two step motors for moving the arms supporting the source and the detector, and (6) an adjustable sample holder that was positioned in the optical center of the diffractometer.

The metal content in the chelating resin was determined by inductively coupled plasma emission spectrometry (ICP-AES) using a VARIAN Liberty 150 spectrometer. Data acquisition and treatment, as well as spectrometer operations, were computer-controlled. A Carlo Erba model EA 1110 CHNS-O analyzer (Carlo Erba Instruments, Milan, Italy) was used for elemental analysis.

Reagents. Mineral acids and iron perchlorates were supplied by Carlo Erba; zinc and chromium perclorates, by Aldrich. Chelex 100 (100−200 mesh) chelating resin in Na form was purchased from Bio Rad (Hercules, CA). Deionized water (ρ > 18 Mohm cm) from a Millipore Milli-Q system was used throughout. Standard Zn(II), Cr(III), and Fe(III) solutions were obtained by dilution from 1 g/L standard AAS solutions (Carlo Erba or Merck).

Preparation of Metal-Loaded Resin. The commercial resin, in Na form, was first well-rinsed in deionized water to remove any extraneous species left by industrial preparation. H_2O (60 mL) was then added to 3 g of the sample, the pH was adjusted to 3−4 with $HClO_4$, and the sample was kept at 75 °C.

The sample was first dried at room temperature for at least 5 days, and then it was heated in an oven at 75 °C for 3 h. By so doing, we obtained the hydrogen form of the resin used as "solvent" in the difference method. The Chelex 100 resin was loaded with Fe(III), Cr(III), and Zn(II), batch-treating the resin in hydrogen form with the desired metal solution. The metal was added gradually up to a total amount in excess of the 1:1 stoichiometric amount for loading all of the iminodiacetic resin groups. The suspension was stirred for about 2 h. After cooling, the metal-loaded resin was rinsed well with water to remove all of the free excess ions, dried at room temperature for at least 5 days, and then oven-dried at 75 °C for 3 h.

Sample Characterization. Metal content in the metal-loaded resin was determined by means of ICP-AES after acid digestion. A 0.035-g portion of the sample, admixed with 3 mL of concentrated HNO_3, was placed on a hot plate at 100−120 °C, and after complete decomposition, it was filtered and transferred into a 50-mL volumetric flask. Analyte was determined using the calibration curve method. Calibration curves were obtained using at least four experimental points. The instrumental parameters were sample flow rate, 2 mL/min; plasma argon flow rate, 15 L/min; auxiliary gas flow rate, 1.5 L/min; integration time for three replicates, 3 s. Different wavelengths (λ) were used, depending on the metal : 275.574 nm (Fe), 357.869 nm (Cr), and 213.856 nm (Zn). All of the standards that were used for calibration curves, as well as the blank, were 0.8 mol/L in HNO_3, to simulate the solution that was produced by sample digestion.

X-ray Scattering Measurements and Data Processing. The spectra were recorded at different fixed θs to obtain the complete q range. q can be written

$$q = 4\pi \sin\theta/\lambda = Ec \sin\theta$$

where q is expressed in $Å^{-1}$ and E, in keV. The value of the constant, c, is 1.014. Operating conditions were as follows: high voltage supply, 45 kV; current, 35 mA; total power, 1535 W; energy range, 22.4 ÷ 42.4 keV; measurement angles (Θ) = 26.0, 15.5, 10.5, 5.0, 3.0, 2.0, 1.5, 1.0, 0.5, and 0.4°; scattering parameter range q = 0.125 ÷ 16.0 $Å^{-1}$.

The experimental data were then corrected[18−20] for the following effects: escape peaks suppression, normalization to the incident radiation intensity, division by X-ray absorption and polarization coefficients, and elimination of contributions due to the Mylar cell and anelastic scattering from the observed intensities I (E, Θ).

Atomic scattering factors, f_h(s), were taken from international tables.[21] The static structure function

$$i(q) = I_{coh}(E,\Theta) - \Sigma f_h^2(q)$$

was then calculated. The radial distribution $D(r)$ is

$$D(r) = 4\pi r^2\rho_0 + 2r\pi^{-1}\int_0^{S_{max}} qi(q)M(q)\sin(rq)\,dq$$

where q is the scattering parameter; ρ_0, the sample's average electronic

(9) Moyers, E. M.; Fritz, J. S. *Anal.Chem.* **1977**, *49*, 418−423.
(10) Atzei, D.; De Filippo, D.; Rossi, A.; Caminiti, R.; Sadun, C. *Spectrochim. Acta* **1995**, *A51* (1), 11.
(11) Atzei, D.; De Filippo, D.; Rossi, A.; Caminiti, R.; Sadun, C. *Inorg. Chim. Acta* **1996**, *248* (2), 203.
(12) Atzei, D.; Sadun, C.; Pandolfi, L. *Spectrochim. Acta* **2000**, *56A*, 531.
(13) Gontrani, L.; Caminiti, R.; Bencivenni, L.; Sadun, C. *Chem. Phys. Lett.* **1999**, *301* (1−2), 131−137.
(14) Caminiti, R.; Carbone, M.; Panero, S.; Sadun, C. *J. Phys. Chem.* **1999**, *103* (4), 10348−10355.
(15) Tromp, R. H.; Neilson, G. W. *J. Phys. Chem.* **1996**, *100*, 7380−7383.
(16) (a) Caminiti, R.; Sadun, C.; Rossi, V.; Cilloco, F.; Felici, R. XXV Italian Congress on Physical Chemistry, Cagliari, Italy, **1991**. (b) Caminiti, R.; Sadun, C.; Rossi, V.; Cilloco, F.; Felici, R. Patent no. RM/93 01261484 June 23, **1993**.
(17) Ballirano, P.; Caminiti, R.; Ercolani, C.; Maras, A.; Orrù, A. *J. Am. Chem. Soc.* **1998**, *120* (49), 12798−12807.
(18) Nishikawa, K.; Iijima, T. *Bull. Chem. Soc. Jpn.* **1984**, *57*, 1750.
(19) Fritsch, G.; Keimel, D. A. *Mater. Sci. Eng.* **1991**, *134A*, 888.
(20) Carbone, M.; Caminiti, R.; Sadun, C. *J. Mater. Chem.* **1996**, *6*, 1709.
(21) International Tables for X-ray Crystallography; Kynoch Press: Birmingham, U.K., 1974; Vol 4.

Table 1. Elemental Analysis Data, Water Content, Densit,y and Stoichiometric Volumes Used for Calculations for Each Chelating Resin

(mol L^{-1})	Chelex 100	Chelex 100 Fe(III)	Chelex 100 Cr(III)	Chelex 100 Zn(II)
M		1.182	1.500	2.066
O	16.585	17.994	19.284	18.800
N	3.813	3.652	3.608	3.595
C	67.864	65.008	64.204	63.977
H	78.744	75.538	76.609	75.857
Water[a]	1.332	3.386	4.854	4.422
V ($Å^3$)[b]	1306.394	1364.032	1380.864	1385.763
d (g L^{-}1)	1206	1258	1268	1328

[a] Included in elemental analysis, determined by thermogravimetry. [b] Stoichiometric volume used in X-ray data treatment.

density ($\rho_0 = [\Sigma_h n_h f_h(0)]^2 V^{-1}$); V ,the stoichiometric unit volume chosen; and $M(q)$, a modification function defined by

$$f_{Fe}^2(0)/f_{Fe}^2(q) \exp(-0.01q^2)$$

The experimental radial distribution functions are shown also as Diff-(r) = $D(r) - 4\pi r^2\rho_0$. Theoretical peaks were calculated by Fourier transformation of the theoretical intensities for the pair interactions

$$i_{ij} = \Sigma f_i f_j \sin(r_{ij}q)(r_{ij}q)^{-1} \exp(-1/2\ \sigma^2_{ij}q^2)$$

using the same sharpening function as for the experimental data and assuming the root-mean-square variation over distance to be $\sigma_{ij.}$ The equipment and technique used are described in detail elsewhere.[16−19]

Results

Analytical results. Elemental analyses confirmed the component percentage of Chelex 100 resin reported in the literature. The elemental component concentrations for the studied samples are listed in Table 1. The relationship between the number of rings substituted by IDA groups and the total number of rings can be found from the C-to-N ratio in the elemental analysis. The number of substituted rings in the resins was found to be 5 of every 8. The C-to-H ratios of the plain resin shown in Table 1 are consistent with the electroneutrality of the hydrogen and salt forms.

WAXS Results. The experimental structure functions show the typical behavior of an amorphous sample. The curves are very similar, exhibiting similar oscillation period and amplitude. This suggests that the metal ion inclusions do not modify the short-range order of Chelex 100 structure. The functions, in the range 0−16 $Å^{-1}$ for Chelex 100 in acidic form and in ionic forms with Fe(III), Cr(III), and Zn(II), respectively, are shown in Figure 1.

The experimental radial distribution function of Chelex 100, in the Diff(r) form, in the range 0−12 Å (Figure 2a) shows peaks at ∼1.45 and 2.45 Å and two large oscillations at greater distances.

The first peaks at 1.45 and 2.45 Å can be attributed to interactions in the Chelex 100 molecule. They represent the distances between the directly bound atoms and between two nondirectly bound atoms. These nonbound distances, like those between atoms 1−3 in the polymer chain or in the benzene ring of the resin matrix, do not depend on molecular conformation.

Figure 2b−d shows the experimental radial distribution functions in the Diff(r) form for the ionic forms of Chelex 100. The presence of the cations does not affect the long-range resin structure, but there are some minor differences in the main short-range peaks, due to the metal ions coordination sphere, which will be described in detail in the following section.

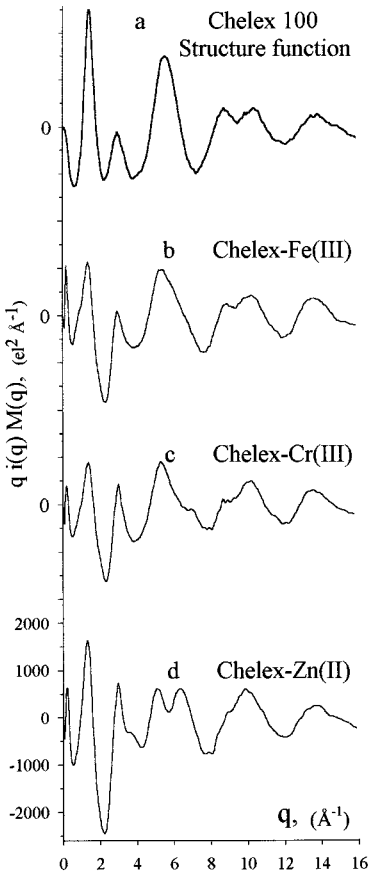

Figure 1. Experimental structure functions in the $qi(q)M(q)$ form: (a) Chelex 100 in acidic form, (b) Chelex 100 loaded with Fe(III), (c) Chelex 100 loaded with Cr(III), (d) Chelex 100 loaded with Zn(II).

Discussion

The structures of metal ion-iminodiacetate ligand complexes in the solid crystal state have been studied elsewhere.[22−24] The IDA ion behaves like a tridentate ligand, chelating metal ions through two carboxylate oxygen atoms and the amine nitrogen atom. The metal ion is bound to one or two IDA ligands in an octahedral arrangement via meridional or facial coordination. There is a moderate preference for facial coordination, although there are a few instances of meridional coordination. When two IDA molecules are coordinated to the metal, fac-trans (N,N) or fac-trans (N,O) is obtained.

Studies of the absorption equilibria of trivalent metal ions indicate that the metal -to-ligand ratio of the complexes formed in the resin phase, which suggests that iron is adsorbed as $(-L^{2-})_2HM^{III}$. This can be rewritten as $(-L^{2-})(-L^{-})M^{III}$ to emphasize the coordination mode. The authors assume that $(-L^{2-})$ coordinates to metal ions using all three of the donor atoms, like iminodiacetate in solution, and $(-L^{-})$ uses only two carboxylates for coordination to the metal ion. The diffraction data have been analyzed under this hypothesis.

A complete structural study of the metal ion−Chelex 100 complex by X-ray diffraction would be very difficult and time-

(22) Subramaniam, V.; Lee, K. W.; Hoggard, P. E. *Inorg. Chim Acta* **1994**, *216*, 155−161.
(23) Crans, D. B.; Jiang, F.; Andreson, O. P.; Miller, S. M. *Inorg. Chem.* **1998**, *37*, 6645−6655.
(24) Caminiti, R.; Cucca, P.; Monduzzi, M.; Saba, G.; Crisponi, G. *J. Chem. Phys.* **1984**, *81* (1), 543−551.

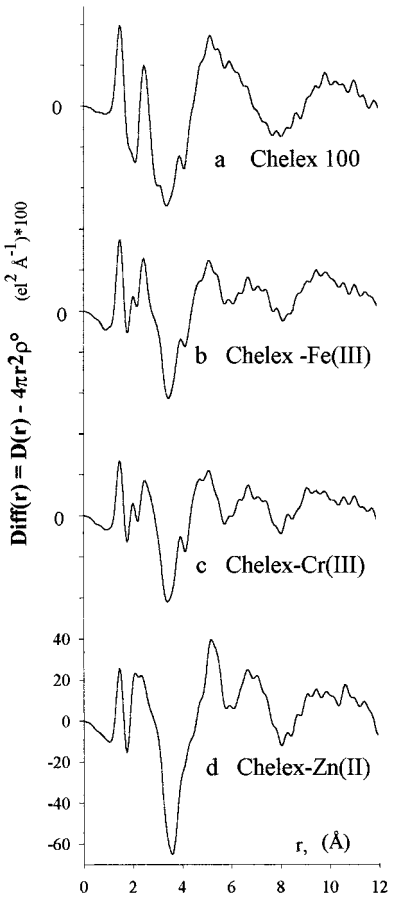

Figure 2. Experimental radial distribution functions in the Diff(r) = $D(r) - 4\pi r^2\rho_o$ form: (a) Chelex 100 in acid form, (b) Chelex 100 loaded with Fe(III), (c) Chelex 100 loaded with Cr(III), (d) Chelex 100 loaded with Zn(II).

consuming. This is because the first coordination distances of the metal ions fall in the range of the resin's second neighbors. They are not dependent on amorphous resin structure, whereas the distances of the second and third coordination sphere are closely related to the resin structure. Thus, it would be necessary to determine the complete resin structure in order to identify which atoms belong to the metal's second coordination sphere.

We have assumed that metals induce only minor disturbances in the resin structure because no substantial differences in the structure functions of Chelex 100, in acid or ionic form, were detected. Thus, we are quite confident in the validity of the difference method. Here, for the first time, we have applied the difference method, previously applied to liquid systems,[13,14] to the resin amorphous system. In a liquid system, the addition of a small amount of solute to obtain a diluted solution does not alter its long- and medium-range structure. Thus, the solute−solute and solute−solvent interactions can be derived by subtracting the structure function of the solvent from that of the solution. In the present case, the resin Chelex 100, in its acid form, has been considered as a solvent. Therefore, we have subtracted a weighted amount of the experimental Chelex 100 structure function, in acid form, from the experimental curves of the Chelex in ionic form. In so doing, we can focus our attention on all new interactions that are present, namely cation−cation and cation−resin interactions. The use of the difference method was necessary because of the great complexity of the resin structure and the small proportion of metal cation, 5−10 wt %, as compared to the resin. In addition, the small amount

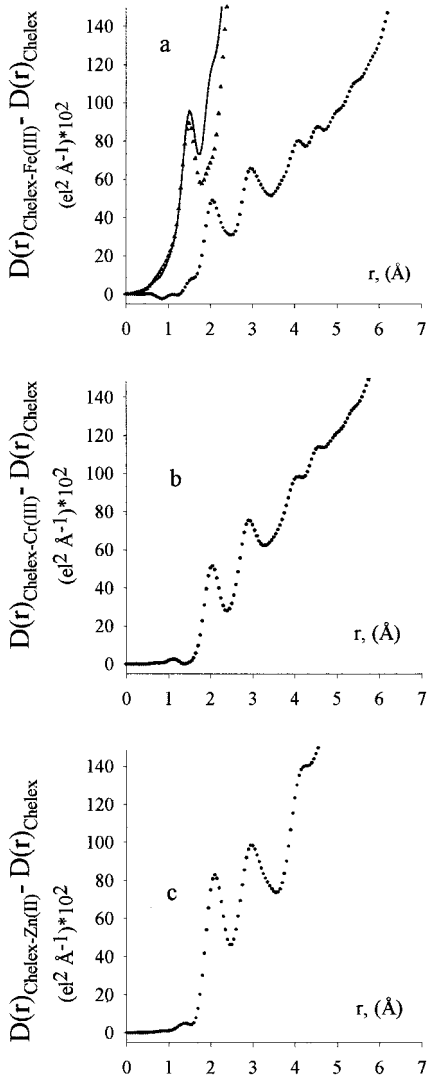

Figure 3. (a) Experimental radial distribution function $D(r)$ of Chelex 100 loaded with Fe(III) (−). Weighted experimental radial distribution function $D(r)$ of Chelex 100 in acidic form (▼), difference curve for the two radial distribution functions, $D(r)_{\text{Chelex−Fe(III)}} - D(r)_{\text{Chelex}}$ (•). (b) Difference curve $D(r)_{\text{Chelex−Cr(III)}} - D(r)_{\text{Chelex.}}$ (c) Difference curve $D(r)_{\text{Chelex−Zn(II)}} - D(r)_{\text{Chelex}}$.

of metal cation allows the determination of the structure of our samples for only a limited range around the metal cation itself.

Therefore, we subtracted a weighted amount of the Chelex 100 acid form distribution radial function $D(r)$ curve from the respective $D(r)$ curve of the Chelex 100 that was loaded with the metal ion. The weighted amount was calculated considering the actual resin content in each sample based on the nitrogen content, that is, 3.652/3.813 for the sample containing Fe(III), 3.608/3.813 for the sample containing Cr(III), and 3.595/3.813 for the sample containing Zn(II). The resulting curve isolates the cation−cation and cation−resin interactions, and it is devoid of contributions of the resin amorphous structure. In Figure 3a, the weighted Chelex 100 and the Fe(III)−Chelex 100 complex experimental $D(r)$ curves and their difference ($D(r)_{\text{Chelex−Fe(III)}}$-$D(r)_{\text{Chelex}}$) are shown. Only the resulting difference curves (the curves of Chelex 100 before and after metal loading have been omitted) of Cr(III) and Zn(II) are plotted in Figure 3b,c. All three difference of the curves show two main peaks located at ∼2.0 and 3.0 Å.

First we analyzed the first peak of the curves. It provided information on the metal-first neighbor interactions, that is, on

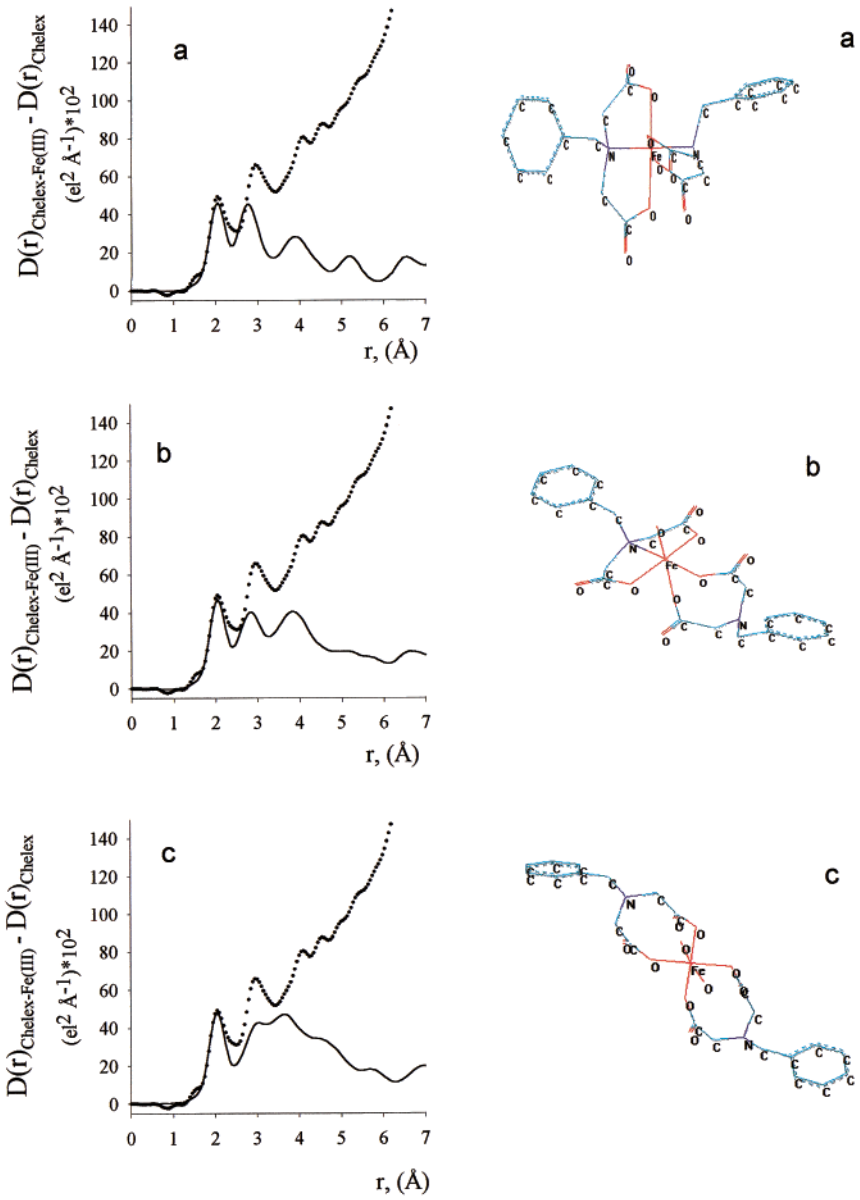

Figure 4. Difference curves for radial distribution functions $D(r)_{\text{Chelex}-\text{Fe(III)}} - D(r)_{\text{Chelex}}$ (•) vs theoretical molecular peak shapes for the shown models (−). All of the models show complexes with 1:2 metal-to-ligand ratios: (**a**) $(-L^{2-})_2H^+$, M^{III}; (**b**) $(-L^{2-})(-L^-)$ H_2O, M^{III} ; (**c**) $(-L^-)_2$ (OH^-) H_2O, M^{III}.

the bound distances; on the coordination numbers; and on the interaction types, metal−oxygen or metal−nitrogen (it is very unlikely that the metal binds through a carbon atom). We found the same coordination for Fe and Cr. Six metal−oxygen interactions, of 2.02 Å, reproduce the first peak. This is in good agreement with literature data on iminodiacetate metal complexes in the solid state and in solution, in which the IDA groups usually coordinate metal by oxygen and nitrogen atoms. In this case, analysis of the first peak alone is not sufficient to determine whether the coordination really takes place by six oxygen or by four oxygen and two nitrogen atoms. The difference between the areas of the peaks we obtained using the first and second model is, in fact, <5%. To establish which atoms are involved in the first coordination sphere, we had to analyze the second peak.

The six atoms of the first metal coordination sphere belong to the resin. They are bound to other atoms constituting the second metal coordination sphere and can generate M−C, M−O, and M−N contributions. Two, three, or even more IDA groups can provide six donor atoms.

Several different structures are possible when two IDA groups bind the metal ion. On the basis of literature data, we have tested the structures suggested. In Figure 4a−c, the experimental radial distribution functions and the theoretical ones, calculated for models involving two IDA groups, are shown. The IDA configurations are such that the second peak of the theoretical functions does not reproduce the experimental ones. Figure 4a refers to two IDA groups, each binding the metal ion through two oxygen atoms and one nitrogen atom. Two IDA groups can be involved in the metal coordination sphere, also through only two oxygen atoms, and the water molecules present in the sample can complete the metal coordination sphere. In this case, the IDA group nitrogen atom can be involved in the second coordination sphere of the metal, but the second theoretical peak is still too small. Figure 4b refers to two IDA groups, one binding the metal ion through two oxygen and one nitrogen atoms, the other through just two oxygen atoms and one water molecule. In Figure 4c, the experimental radial distribution function is compared to the theoretical one involving two IDA groups and two water molecules. The above figures refer to

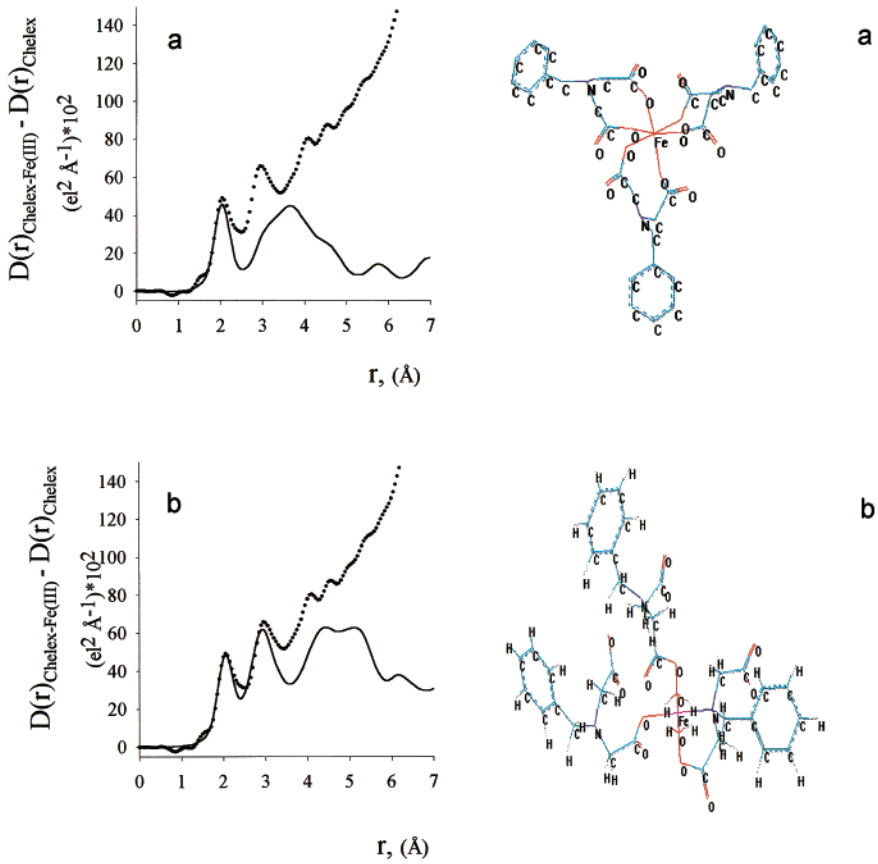

Figure 5. Difference curves for radial distribution function $D(r)_{\text{Chelex}-\text{Fe(III)}} - D(r)_{\text{Chelex}}$ (•) vs theoretical molecular peak shapes for the shown models (−). All of the models show complexes with 1:3 metal-to-ligand ratios: (**a**) $(-L^{-})_3$, M^{III}; (**b**) $(-L^{-})_2$ $(-L^{2-})H^{+}$ H_2O, M^{III}.

one of the possible configurations that the ligand oxygen atoms can take around the metal ion. We also tested the other models, and the results obtained were equally unsatisfactory.

In Figure 5a,b, the experimental radial distribution functions are compared to the theoretical ones involving three IDA groups. In Figure 5a, the three ligands are in the anionic form ($-LH^{-}$) and a 1:3 complex is represented. In Figure 5b, three ligands are involved in the metal ion coordination, two through only one carboxylate oxygen atom, the other through one carboxylate oxygen and the nitrogen atom. Two water molecules complete the metal coordination sphere.

The second peak in the experimental radial distribution function is reproduced only when four IDA groups are coordinated to the metal ion by four oxygen atoms supplied by four different IDA groups, and the two remaining coordination sites are occupied by water molecules (see model shown in Figure 6). The experimental difference curves for the systems with Fe(III) and Cr(III) and the theoretical ones based on the proposed model are shown in Figure 6a,b, respectively.

Several samples of Chelex in ionic form with Fe(III) were prepared and analyzed; the metal content ranged from 1.182 to 1.666. The proposed model is valid for these samples, as well as for the detailed one.

The model, which holds for Fe(III) and Cr(III), is not suitable for Zn(II) (see Figure 7). It is well-known[25−28] that the Zn(II) cation can be coordinated in an octahedral or tetrahedral arrangement. We assumed that, in the absence of water molecules, two IDA groups could coordinate Zn(II) with tetrahedral configuration. The theoretical distribution function, assuming that the tetrahedral model holds, and the experimental one are shown in Figure 8. The first peak of the theoretical function is lower than the experimental one, indicating that four M−O contributions are not sufficient to reproduce it.

Careful examination of the experimental function showed that the first peak is not symmetric. The peak can be considered the result of similar, but not equal, contributions from two distances. Different hypotheses have been advanced for determining the best configuration. Five Zn−O contributions, three at 2.08 Å and two at 2.16 Å, nicely reproduce the peak.

To our knowledge, a triangular bipyramidal structure for the Zn(II) complexes has not been reported elsewhere. Moreover, this configuration would imply that the metal coordinating IDA groups differentiate between two oxygen atoms of the acetate group. We assumed that IDA groups coordinating the Zn(II) maintain their conformation unchanged, as happens when they coordinate Fe(III) and Cr(III). The best-fit model appears to be achieved when the Zn(II) has roughly 50% tetrahedral arrangement with Zn−O distances of 2.16 Å and 50% octahedral configuration with distances of 2.08 Å and includes two water molecules, as shown in Figure 9.

The good agreement between the experimental radial function and the theoretical one that was calculated using this model for the second peak confirms this hypothesis. However, it is already known that the Zn(II) ion can exhibit two coordination structures simultaneously.[29]

The proposed model is compatible with IDA density in the resin phase, and the low degree of polymerization can permit

(25) Guevara-Garcia, J. A.; Barba-Behrens, N.; Tapia-Benavides, A. R.; Rosales-Hoz, M. J.; Contreras, R. *Inorg. Chim. Acta* **1995**, *239*, 93−97.
(26) Constable, E. C. *Coord. Chem. Rev.* **1984**, *58*, 1−5.
(27) Fuertes, A.; Miravitlles, C.; Molins, E.; Escrivá, E.; Beltran, D. *Acta Crystallogr.* **1986**, *42C*, 421−425.
(28) Atzei, D.; Caminiti, R.; Sadun, C.; Bucci, R.; Corrias, A. *Phosphorus, Sulphur Silicon Relat. Elem.* **1993**, *79*, 13−24.
(29) Irish, D. E.; Jarv, T. *Appl. Spectrosc.* **1983**, *37* (1), 50−55.

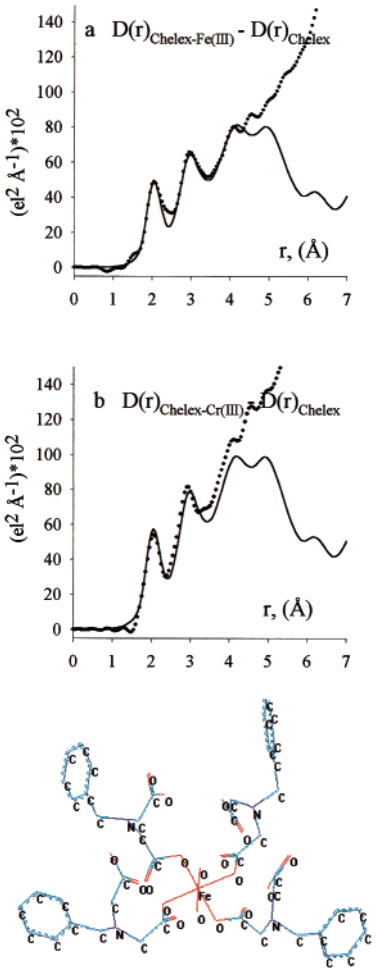

Figure 6. (a) Difference curve for radial distribution function $D(r)_{\text{Chelex}-\text{Fe(III)}} - D(r)_{\text{Chelex}}$ (•) vs theoretical molecular peak shapes for the shown model (−). (b) Difference curve for radial distribution function $D(r)_{\text{Chelex}-\text{Cr(III)}} - D(r)_{\text{Chelex}}$ (•) vs theoretical molecular peak shapes for the shown model (−).

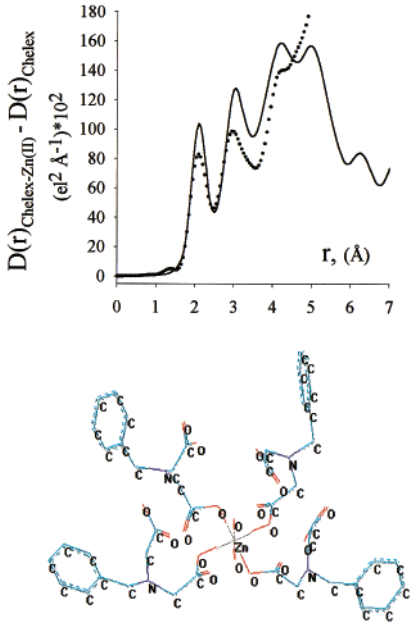

Figure 7. Difference curve for radial distribution function $D(r)_{\text{Chelex}-\text{Zn(II)}} - D(r)_{\text{Chelex}}$ (•) vs theoretical molecular peak shapes for the octahedral model (−).

favorable orientation of the IDA groups. The metal loading carried out at pH 4 suggests that the main species for the IDA group is in the zwitterionic form. Because no perchlorates ions were detected in the resin phase, electroneutrality was maintained, because the resin loses three H^+/metal ion.

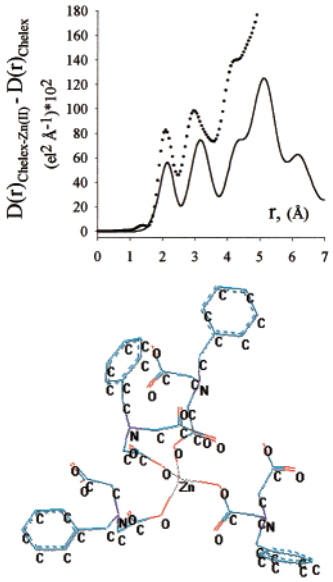

Figure 8. Difference curve for radial distribution function $D(r)_{\text{Chelex}-\text{Zn(II)}} - D(r)_{\text{Chelex}}$ (•) vs theoretical molecular peak shapes for the tetrahedral model (−).

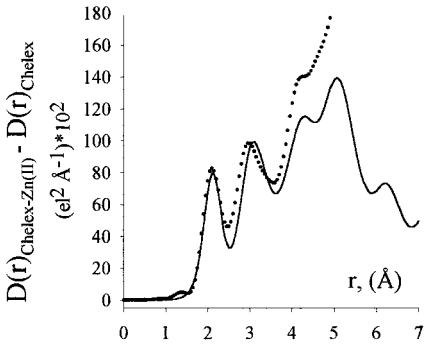

Figure 9. Difference curve for radial distribution function $D(r)_{\text{Chelex}-\text{Zn(II)}} - D(r)_{\text{Chele,}}$ (•) vs 50% of theoretical molecular peak shapes for the octahedral model and 50% for the tetrahedral model (−).

Conclusions:

The results of this study demonstrate that the difference method used for solutions can be advantageously applied to solid amorphous systems. In the case at hand, the use of this method simplified the study of the system. Indeed, the amorphous solid structure can be considered to be a matrix, because it preserves its medium- and long-range structure after inclusion of metal ions. Metal ion neighbors can be easily determined with this method.

The study of the coordination structure of metal ions with chelating groups having a polymeric structure of considerable dimensions is complicated by the complex amorphous structure of the polymer itself. The possibility of disregarding the resin structure simplifies the work, allowing reliable metal coordination structures to be obtained. The proven validity of the differences method for this kind of system will enable more complex systems to be studied, like those composed of particular metal-IDA complexes with some resin and oxyanions such as selenite and tellurite.

JA0003728